Available online at www.sciencedirect.com
SCIENCE DIRECT
Journal of Photochemistry and Photobiology A: Chemistry 178 (2006) 258–263
Journal of Photochemistry and Photobiology A:Chemistry
www.elsevier.com/locate/jphotochem

Quantum control of molecular chirality: Ab initio molecular orbital study and wave packet analysis of l,l′-binaphthyl

Kunihito Hoki [a], Shiro Koseki [b], Takeshi Matsushita [b], Riadh Sahnoun [c], Yuichi Fujimura [c,*]

[a] *Department of Chemistry, University of Toronto, Toronto, Canada*
[b] *Department of Chemistry, Graduate School of Science, Osaka Prefecture University, Osaka 599-8531, Japan*
[c] *Department of Chemistry, Graduate School of Science, Tohoku University, Sendai 980-8578, Japan*

Available online 11 November 2005

This paper is dedicated to Professor Iwao Yamazaki.

Abstract

The results of a theoretical study on quantum control of an axial chirality change reaction in l,l′-binaphthyl are presented. The chiral change from the **P** form to the **M** form via the third excited electronic state has been considered, the pure enantiomer of the **P**-form being assumed as the initial state. Asymmetric double-well potential energy surfaces of the ground state (S_0) and the third excited electronic state (S_3) and the corresponding transition moment along the reaction coordinate were evaluated using ab initio MO methods. An optimal control theory was applied to the chirality change reaction. The results of the quantum control showed that motions of nuclear wavepackets on both the S_0 and S_3 reaction coordinates were controlled. The mechanism of the quantum control is explained as a sequence of quantum transitions between S_0 and S_3, and the control is performed by irradiating a sequence of a pump-dump pulse.

Keywords: Quantum control; Molecular chirality; Binaphthyl; Wave packet; Isomerization

1. Introduction

Molecular chirality plays important roles in various research areas in chemistry and biochemistry [1,2]. It is well known that chiral molecules are selectively manipulated by photoreactions of racemic mixtures that are equal mixtures of two chiral forms by irradiation of circularly polarized laser light [3]. However, its enantiomer excess is very low. With recent developments in laser science and technology, much interest has been shown in quantum control of chemical reaction dynamics [4–12]. The effectiveness of quantum control originates from the fact that wave functions relevant to reaction dynamics are directly controlled through a coherent interaction between the molecule of interest and laser fields. Electric fields of laser pulses can now be designed using pulse shaper techniques with an adaptive feedback algorithm [13–17].

Theoretical studies on quantum control of molecular chirality have been carried out by several groups [18–34]. In a previous paper [35], we presented results of a theoretical study on quantum control of a chiral exchange reaction of difluorobenzo[c]phenanthrene by using infrared laser pulses. In this paper, we present a scenario for quantum control of an axial chirality control reaction in l,l′-binaphthyl (referred to simply as binaphthyl in the following discussion) using UV lasers; the nuclear wave packet motion on both the ground and electronic excited states is manipulated by using UV laser pulses. UV laser pulses are better than IR laser pulses for quantum control of reaction dynamics especially when a transition state of a chiral exchange reaction has a high-energy barrier in the ground state.

In the present study, we investigated an axial-chirality exchange reaction from the **P** (or **M**) form to the **M** (or **P**) form in binaphthyl. This axial-chirality exchange reaction can also be considered as an isomerization. The ground and excited state potential surfaces and the transition moment functions between them were evaluated by using ab initio molecular orbital (MO) methods. The isomerization does not have a symmetric potential energy surface along a reaction path. The potential energy

* Corresponding author. Tel.: +81 22 795 7715.
E-mail addresses: shiro@ms.cias.osakafu-u.ac.jp (S. Koseki), fujimura@mcl.chem.tohoku.ac.jp (Y. Fujimura).

1010-6030/$ – see front matter © 2005 Elsevier B.V. All rights reserved.
doi:10.1016/j.jphotochem.2005.09.029

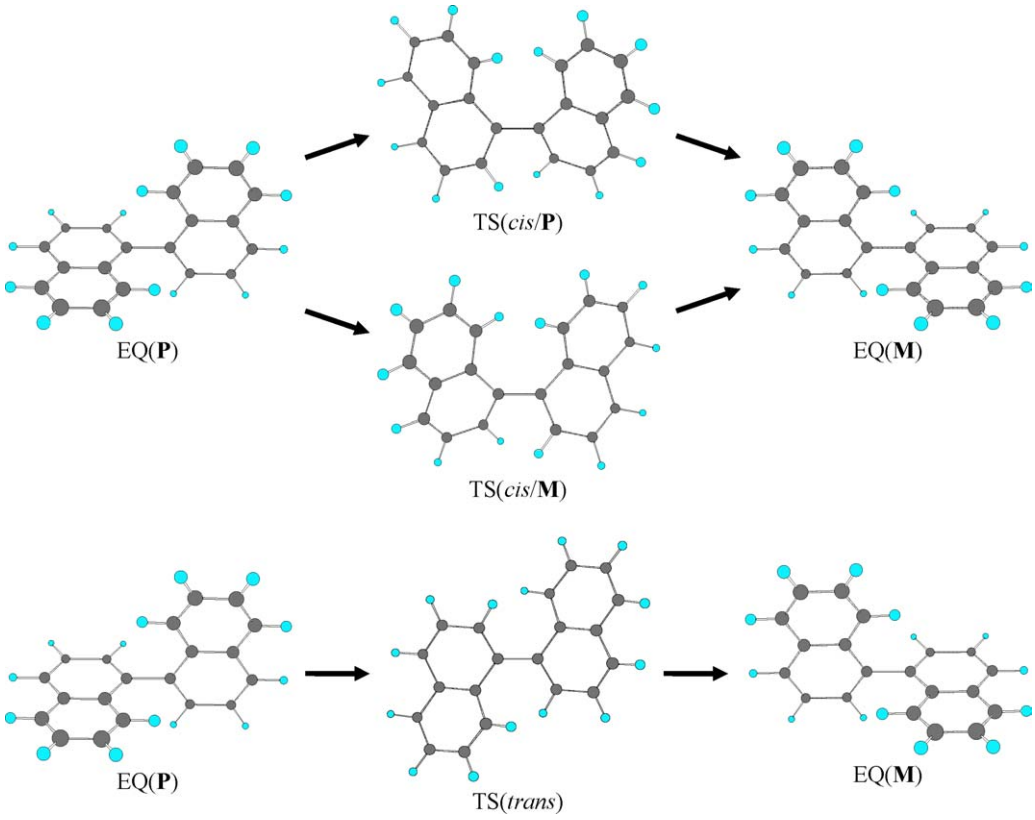

Fig. 1. Stationary structures along the isomerization of binaphthyl via TS(*cis*) (top part) and TS(*trans*) (bottom part).

surfaces also have several wells along the reaction path. An optimal quantum control theory was applied to molecular-chilarity exchange reaction that proceeds on such relatively complicated potential surfaces. The results showed that the motion of nuclear wave packets can be controlled by consecutive electronic transitions, and the transitions are induced by using a pump-dump pulse sequence.

In Section 2, we present results of ab initio MO studies on binaphthyl. In Section 3, we present results of optimal control of the axial-chirality exchange reaction and wave packet analysis.

2. Ab initio molecular orbital studies

Stationary structures on the potential energy surface of the ground state in binaphthyl were optimized using the RHF/6-31G(d,p) method [36]. The equilibrium structures, EQ(**P**) and EQ(**M**), are illustrated in Fig. 1. The reaction path is defined by the intrinsic reaction coordinate (IRC) at this computational level of theory. The total energies of the low-lying electronic states along the IRC were calculated on the basis of the more reliable MCSCF + FOCI level of theory, where the MCSCF active space includes four occupied and four vacant orbitals close in energy to the HOMO and LUMO. The total energies are plotted against the dihedral angle $C_2 - C_1 - C_1' - C_2'$ at each point along the IRC in Fig. 2 (see Scheme 1). The transition moments among these states were also computed at this level of theory. Table 1 shows the relative energies of the stationary structures along the IRC. The stationary structures and their relative energies are in good agreement with the results reported by other groups [37].

The top part of Fig. 1 illustrates the isomerization paths via the *cis* configuration: the transition state TS(*cis*) has C_2 symmetry and has an optical isomer. They are referred to have as TS(*cis*/**P**) and TS(*cis*/**M**). Accordingly, two paths must exist for the isomerization: (1) EQ(**P**), for example, climbs up the relatively gentle slope of the potential energy curve in the ground state and goes through TS(*cis*/**P**) to reach EQ(**M**) and (2) EQ(**P**) climbs up the very steep slope and goes through TS(*cis*/**M**) to reach EQ(**M**). This fact indicates that there are at least two important vibrational motions, rotation around the inter-ring C–C bond and C–H bending motions near the inter-ring C–C bond. The selection of the isomerization paths depends on which motion is promoted at the initial stage of reaction. According to the results of our previous investigation [35], it is much easier to control the reaction by an optimal laser field when the steeper motion is promoted first.

Table 1
Relative energies (kcal/mol) of stationary structures

	EQ	TS(*cis*)	TS(*trans*)
Symmetry	C_2	C_2	C_1
RHF	0	39.8	30.2
MCSCF	0	38.5	29.5
MCSCF + FOCI	0	38.6	29.4

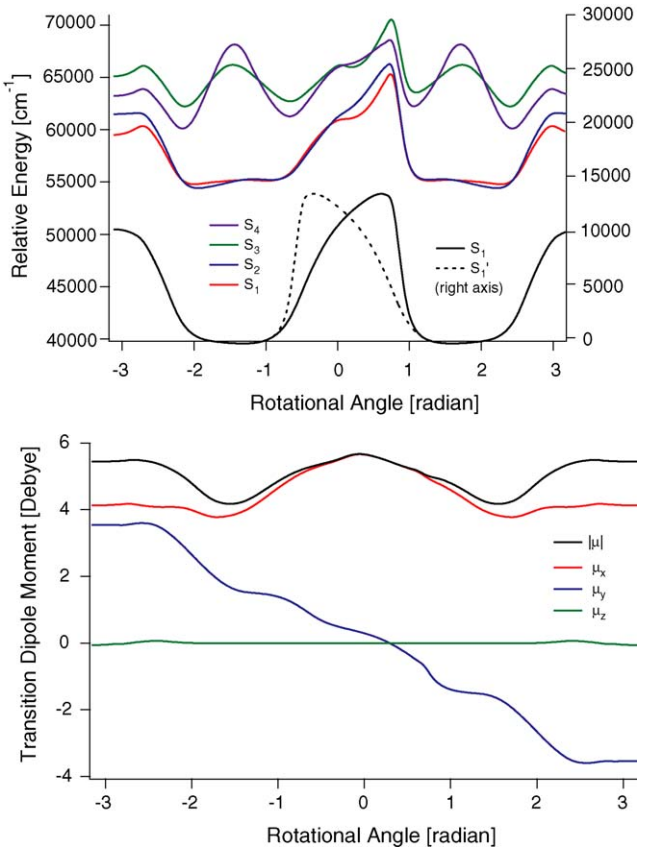

Fig. 2. Potential energy curves of low-lying states obtained using the MCSCF + FOCI method (top part). Absolute values of transition dipole moment vectors for the excitation from S_0 (middle part). The x, y and z components of the transition moment vector from S_0 to S_3 (bottom part).

The bottom part of Fig. 1 shows the isomerization paths via the *trans* configuration: in finding the true transition state, it is revealed that the C_{2h} (planar) optimized structure has three imaginary frequencies, so that this is not the transition state. The C_2 optimized structure is also not the transition state because of two imaginary frequencies. Finally, an asymmetrical structure, TS (*trans*), is proved to be the true transition state for the chirality exchange reaction via the *trans* configuration. Surprisingly, even though TS(*trans*) has two naphthalene rings with different structures, it does not have an optical isomer: its mirror image completely overlaps the original one. Therefore, there is only one path along the chirality exchange reaction via the *trans* configuration. The molecular symmetry C_2 disappears somewhere before it reaches TS(*trans*) and, after it passes through TS(*trans*), the molecular symmetry appears before it reaches EQ. As a result, the potential energy curve of the ground state is symmetric about TS(*trans*) (see the top part of Fig. 2). It is also very interesting that the TS (*trans*) is the point of the chirality change reaction.

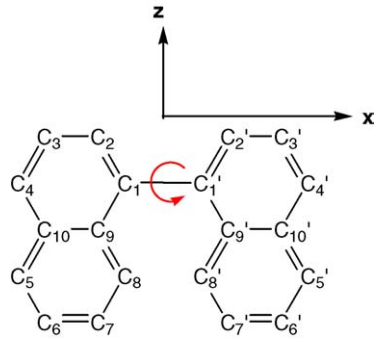

Scheme 1.

We now assume that the dihedral angle $C_2 - C_1 - C_1' - C_2'$, (see Scheme 1) is the reaction coordinate ϕ for the chirality exchange reaction. Accordingly, the equilibrium structures, EQ(**P**) and EQ(**M**), appear at $\phi \sim 90^\circ = \pi/2$, and TS(cis/**P**) and TS(cis/**M**) have $\phi = \pm 26.4^\circ$, while $\phi = 180^\circ = \pi$ for TS(*trans*). As stated above, since it is easier to control the chirality exchange reaction when the steeper motion is promoted first, the path EQ(**P**) → TS(*cis*/**M**) or EQ(**M**) → TS(*cis*/**P**) should be employed instead of the path EQ(**P**) → TS(*cis*/P) or EQ(**M**) → TS(*cis*/M) (see the broken line labeled as S_0' in the top part of Fig. 2). Namely, the reaction path is assumed to be

$$\text{EQ(\textbf{P})} \leftarrow \text{TS}\,(cis/\textbf{P}) \leftarrow \text{EQ(\textbf{M})} \rightarrow \text{TS}(trans) \rightarrow \text{EQ(\textbf{P})}$$

and/or

$$\text{EQ(\textbf{M})} \leftarrow \text{TS}\,(cis/\textbf{M}) \leftarrow \text{EQ(\textbf{P})} \rightarrow \text{TS}(trans) \rightarrow \text{EQ(\textbf{M})}.$$

These two paths have potential energy curves depicted by a solid line in the top part of Fig. 2. Along this path, several electronically excited states were calculated at the MCSCF + FOCI level of theory, and the transition moments between the ground state and these excited states were also computed using these wave functions. The largest transition moment is obtained for the excitation from the ground state to the third excited state S_3 (see the middle part of Fig. 2).

The character of the third excited state S_3 is described here: since binaphthyl has two naphthalene rings, all of the π orbitals can be said to be quasi-degenerate. Therefore, when the present discussion employs the naphthalene π orbitals themselves, both the first and second excited states, S_1 and S_2, have a combination of the excitations from the highest occupied molecular orbitals (HOMOs) to the next-lowest unoccupied molecular orbitals (NLUMOs) and those from the next-highest occupied molecular orbitals (NHOMOs) to the lowest unoccupied molecular orbitals (LUMOs). Both the third and fourth excited states, S_3 and S_4, have excitation from the HOMOs to LUMOs as their main configuration. This reverse energetic order is caused by the fact that naphthalene belongs to alternant conjugated hydrocarbons and its lowest excited state has a linear combination of HOMO–NLUMO and NHOMO–LUNO single excitations, instead of HOMO–LUMO excitation. This is the reason why S_3 (or S_1) is energetically close to S_4 (or S_2) along the whole chirality exchange reaction path.

3. Optimal control of chirality exchange reaction and wave packet analysis

We consider a molecular chirality change from EQ(**P**) to EQ(**M**) via the S_3 state of binaphthyl, since the excitation from S_0 to S_3 has a large transition moment compared with those from

S_0 to other electronically excited states. For simplicity, we omit effects of nonadiabatic coupling between these two states. An electric field vector of laser pulses is assumed to be parallel to the x-axis.

The time evolution of binaphthyl expanded in terms of the ground and excited electronic states is determined by the time-dependent Schrödinger equation,

$$i\bar{h}\frac{\partial}{\partial t}\begin{pmatrix}\psi_g(\phi,t)\\ \psi_e(\phi,t)\end{pmatrix} = \begin{pmatrix}\hat{h}_g & -\mu_{ge}(\phi)E(t)\\ -\mu_{eg}(\phi)E(t) & \hat{h}_e\end{pmatrix} \times \begin{pmatrix}\psi_g(\phi,t)\\ \psi_e(\phi,t)\end{pmatrix}. \quad (1)$$

Here, $\mu_{ge}(\phi)$ is x component of the transition dipole moment vector, $E(t)$ is the x component of the electric field vector of the laser, $\Psi_g(\phi,t,)$ and $\Psi_e(\phi,t,)$ are nuclear wave packets in the S_0 and S_3 states, respectively, and $\hat{h}_g$ and $\hat{h}_e$ are nuclear Hamiltonians in the S_0 and S_3 states, respectively. The nuclear Hamiltonians h_g and h_e is written as $\hat{h}_g = -(\bar{h}^2/2I)(\partial^2/\partial\phi^2) + V_g(\phi)$ and $\hat{h}_g = -(\bar{h}^2/2I)(\partial^2/\partial\phi^2) + V_e(\phi)$ respectively, where ϕ corresponds to a dihedral angle between two naphthyl rings, I (=350 amu Å^2) is the moment of inertia, and V_g (ϕ) and $V_e(\phi)$ are the potential energy functions of S_0 and S_3 states shown in the top in Fig. 2, respectively.

In the optimal quantum control theory [12], the optimal electric field $E(t)$ is determined by the expression

$$E(t) = -AIm < X(t)|\mu|\psi(t) >, \quad (2)$$

where A is a weighting factor. Here, $|X(t)>$ satisfies the time-dependent Schrödinger equation whose Hamiltonian is given as $\hat{H}(t)$

$$i\bar{h}\frac{\partial}{\partial t}|X(t)>= \hat{H}(t)|X(t)>, \quad (3)$$

with the final condition at $t = t_f$ $|X(t_f)> = W|\Psi(t_f)>$. W is the target operator.

The optimal electric field $E(t)$ was derived by using a monotonically convergent iteration algorithm developed by Zhu and Rabitz [13]. We set the ground eigenstate as the initial state and $t_f = 3$ ps as the final time of quantum control. We set a projection operator consisting of the lower 30 eigenstates of the EQ(**M**) as the target operator W, which makes the wave packet localized near the equilibrium position of the EQ(**M**).

The top part of Fig. 3 shows the optimal electric field designed for the molecular chirality change reaction from EQ(**P**) to EQ(**M**) via the S_3 state in binaphthyl. The electric field consists of a sequence of pump–dump pulses as shown in Fig. 4. The middle part of Fig. 3 shows a time-frequency resolved spectrum of the optimal electric field. The frequency range of the designed electric field is located between 50,000 and 65,000 cm^{-1} and corresponds to the energy gap between S_0 and S_3. The bottom part of Fig. 3 shows the time evolution of population $P_g(t)$ in the S_0 state and $P_e(t)$ in the S_3 state. We can see from the bottom part of Fig. 3 that the population is transferred between S_0 and S_3 many times and that 89% of the population is localized near EQ(**M**) at the final time $t_f = 3$ ps. Such an effective localization

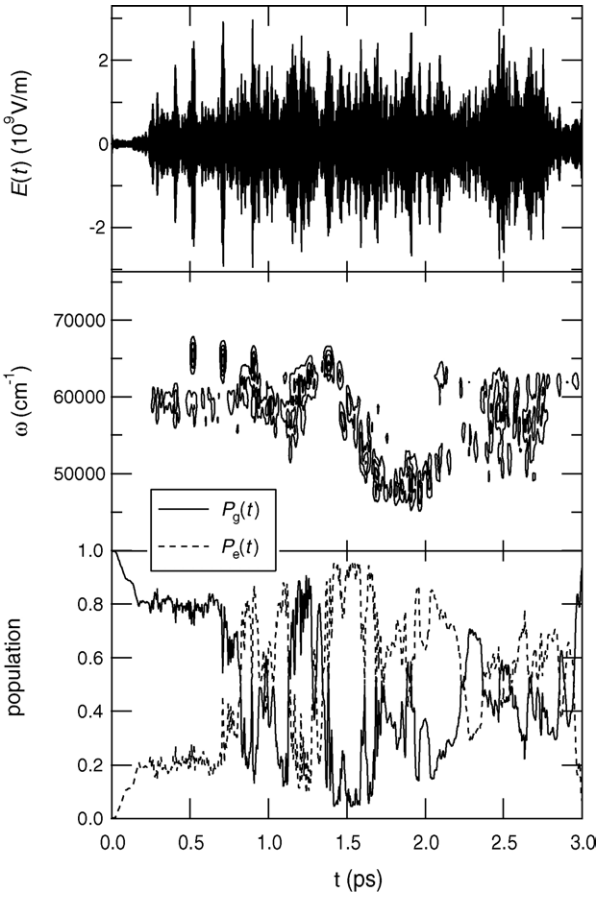

Fig. 3. The optimal electric field of laser pulses designed by a quantum control procedure (top part). Time–frequency resolved spectrum of the optimal electric field (middle part). Time propagation of populations $P_g(t)$ and P_e(t) (bottom part).

in the population indicates the validity of the quantum control procedure.

The middle and bottom parts in Fig. 4 show the wave packet propagation on the reaction path in the S_3 state and that in the S_0 state, respectively. The top part of Fig. 4 shows the control mechanism in which a sequence of pump–dump pulses is operative. This figure clearly indicates that the pump and dump pulses effectively control the chirality change reaction on the two asymmetric potential surfaces. We can see that the optical transitions induced by the pump and dump pulses satisfy the Franck-Condon principle, i.e., the nuclear wave packets are transferred on the two electronic states under the condition of their nuclear position and linear momentum.

It should be noted that this high yield obtained in the present chirality control is brought about within the adiabatic approximation. Inclusion of nonadiabatic couplings into the reaction scheme reduces its yield. Quantum control of photochemical reactions that takes into account nonadiabatic couplings has been presented elsewhere [38–40]. It would be interesting to apply the quantum control method that takes into account nonadiabatic couplings to the present chirality change reaction.

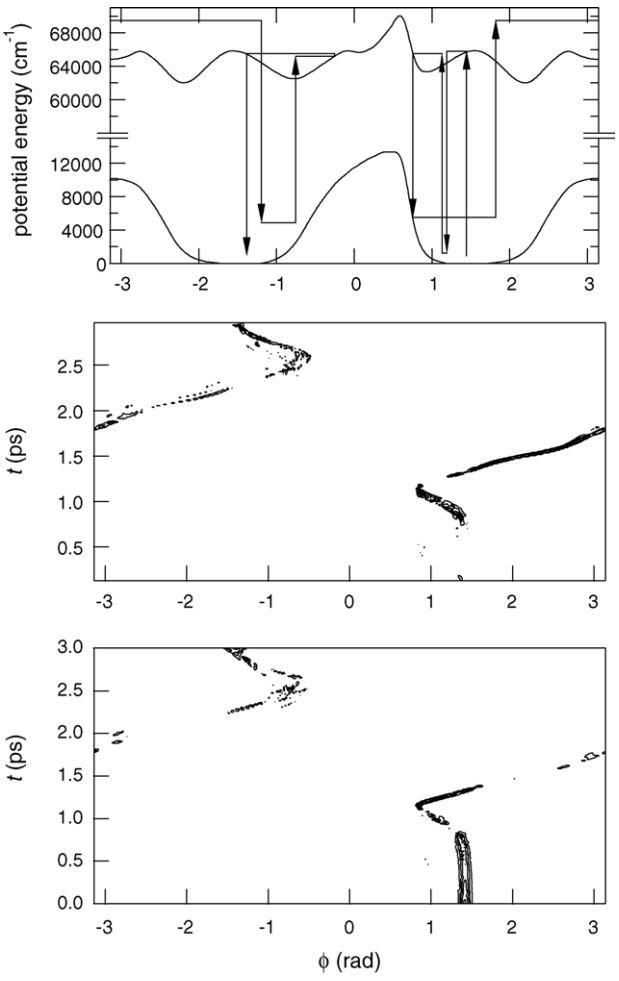

Fig. 4. The pump–dump mechanism of the quantum control (top part). Time propagation of wave packets on S_3 and S_0 (middle and bottom parts), respectively.

4. Summary

We have presented the results of a theoretical study on quantum control of an axial chirality change reaction in binaphthyl. As an example, we have considered the chiral change from EQ(**P**) to EQ(**M**) via the third excited electronic state. The potential energy surfaces of the ground and third excited electronic states and the corresponding transition moment along the reaction coordinate were evaluated using ab initio MO methods. The potential energy surface along a reaction coordinate of the chirality change of the molecular chirality is not symmetric. The results of quantum control were analyzed in terms of nuclear wave packet propagation on both the ground and excited states. The results showed that the motion of nuclear wave packets on asymmetric double-well potential in S_0 and complicated potential surface in S_3 were sufficiently controlled by a sequence of transitions between the S_0 and S_3 states and that the control is carried out by a pump–dump pulse sequence.

Assuming the pure enantiomer of the **P** form of binaphthyl, we have treated laser control of molecular chirality change from the **P** form to the **M** form. It should be noted that the designed optimal pulse can also produce the **P** form if the **M** form is the initial state. In a racemic mixture of the **M** and **P** forms in which the molecular chirality changes from the **P** form to the **M** form while the **M** form is maintained through the laser control, a quantum control of molecular chirality can be achieved by using two-dimensional polarizations of an electric field with a pre-oriented conformation [27,28,30,31].

Acknowledgements

This work was partly supported by a Grant-in-Aid for Scientific Research on Priority Areas, “Control of Molecules in Intense laser Fields” from the MEXT of the Japanese Government (No. 14077215) and by a Grant-in-Aid for Scientific Research (B) (No. 17350004). R.S. acknowledges the receipt of a JSPS grant (P02353).

References

[1] B.M. Avalos, R. Babiano, P. Cintas, J. Jimenez, J.C. Palacios, L.D. Barron, Chem. Rev. 98 (1998) 2391–2662.
[2] R. Noyori, Asymmetric Catalysis in Organic Synthesis, Wiley, New York, 1994.
[3] Y. Inoue, Chem. Rev. 92 (1992) 741–770.
[4] Y. Fujimura, L. González, K. Hoki, J. Manz, Y. Ohtsuki, H. Umeda, in: R.J. Gordon, Y. Fujimura (Eds.), Quantum Control of Molecular Reaction Dynamics, Adv. in Multi-photon Processes and Spectroscopy, 14, World Scientific, Singapore, 2001, pp. 30–46.
[5] P. Brumer, M. Shapiro, Annu. Rev. Phys. Chem. 43 (1992) 257–282.
[6] R. Judson, H. Rabitz, Phys. Rev. Lett. 68 (1992) 1500–1503.
[7] E.D. Potter, J.L. Herek, S. Pedersen, Q. Liu, A.H. Zewail, Nature 355 (1992) 66–68.
[8] B. Kohler, J.L. Krause, F. Raksi, K.R. Wilson, V.V. Yakovlev, R.M. Whitnell, Y.J. Yan, Ace. Chem. Res. 28 (1995) 133–140.
[9] L. Zhu, V. Kleiman, X. Li, S.P. Lu, K. Trentelman, R.J. Gordon, Science 270 (1995) 77–80.
[10] R. Kosloff, S.A. Rice, P. Gaspard, S. Tersigni, D.J. Tannor, Chem. Phys. 139 (1989) 201–220.
[11] M. Sugawara, Y. Fujimura, J. Chem. Phys. 100 (1994) 5646–5655.
[12] R.A. Gordon, Y. Fujimura, Encyclopedia of Physical Science and Technology, Academic Press, San Diego, 2002, pp. 207–231.
[13] W. Zhu, H. Rabitz, J. Chem. Phys. 109 (1998) 385–391.
[14] B. Assion, T. Baumert, M. Bergt, T. Brixner, B. Kiefer, V. Seyfried, M. Strehle, G. Gerber, Science 282 (1998) 919–922.
[15] H. Rabizt, R. de Vivie-Riedle, M. Motzkus, K. Kompa, Science 288 (2000) 824–828.
[16] R.J. Levis, G.M. Menkir, H. Rabitz, Science 292 (2001) 709–713.
[17] G. Vogt, G. Krampert, P. Niklaus, P. Nuernberger, G. Gerber, Phys. Rev. Lett. 94 (2005), pp. 068305-1–068305-4.
[18] M. Shapiro, P. Brumer, J. Chem. Phys. 95 (1991) 8658–8661.
[19] J.A. Cina, R.A. Harris, J. Chem. Phys. 100 (1994) 2531–2536.
[20] A. Salam, W.J. Meath, J. Chem. Phys. 106 (1997) 7865–7868.
[21] J. Shao, P. Hänggi, J. Chem. Phys. 107 (1997) 9935–9941.
[22] M. Shapiro, E. Frishman, P. Brumer, Phys. Rev. Lett. 84 (2000) 1669–1672.
[23] D. Gerbasi, M. Shapiro, P. Brumer, J. Chem. Phys. 115 (2001) 5349–5352.
[24] Y. Fujimura, L. González, K. Hoki, J. Manz, Y. Ohtsuki, Chem. Phys. Lett. 306 (1999) 1–8.
[25] Y. Fujimura, L. González, K. Hoki, D. Kröner, J. Manz, Y. Ohtsuki, Angew. Chem. Int. Ed. 39 (2000) 4586–4588.
[26] K. Hoki, Y. Ohtsuki, Y. Fujimura, J. Chem. Phys. 114 (2000) 1575–1581.
[27] L. González, D. Kröner, I.R. Solá, J. Chem. Phys. 115 (2001) 2519–2529.

[28] K. Hoki, Y. Fujimura, in: A.D. Bandrauk, R.J. Gordon, Y. Fujimura (Eds.), Laser Control and Manipulation of Molecules, American Chemical Society, 2001, pp. 32–46.
[29] K. Hoki, Y. Fujimura, Chem. Phys. 267 (2001) 187–193.
[30] K. Hoki, L. González, Y. Fujimura, J. Chem. Phys. 116 (2002) 2433–2438.
[31] K. Hoki, L. González, Y. Fujimura, J. Chem. Phys. 116 (2002) 8799–8802.
[32] Y. Ohta, K. Hoki, Y. Fujimura, J. Chem. Phys. 116 (2002) 7509–7517.
[33] Y. Fujimura, Recent Res. Devel. Chem. Phys. 4 (2003) 345–358.
[34] D. Kröner, L. González, Chem. Phys. 298 (2004) 55–63.
[35] H. Umeda, M. Takagi, S. Yamada, S. Koseki, Y. Fujimura, J. Am. Chem. Soc. 124 (2002) 9265–9271.
[36] M.W. Schmidt, K.K. Baldridge, J.A. Boatz, S.T. Elbert, M.S. Gordon, J.H. Jensen, S. Koseki, N. Matsunaga, K.A. Nguyen, S. Su, T.L. Windus, M. Dupuis, J.A. Montgomery Jr., J. Comput. Chem. 14 (1993) 1347–1363.
[37] V. Setnicka, M. Urbanova, P. Bour, V. Karl, K. Volka, J. Phys. Chem. A 105 (2001) 8931–8938.
[38] R. de Vivie-Riedle, K. Sundermann, M. Motzkus, Faraday Discuss. 113 (1999) 303–317.
[39] Y. Ohtsuki, K. Ohara, M. Abe, K. Nakagami, Y. Fujimura, Chem. Phys. Lett. 369 (2003) 525–533.
[40] M. Abe, Y. Ohtsuki, Y. Fujimura, W. Domcke, in: T. Kobayashi, T. Okada, T. Kobayashi, K.A. Nelson, S. De Silverstri (Eds.), Ultrafast Phenomena XIV, Springer, Berlin, 2004, pp. 613–615.